

Hierarchical Porous NiCo₂O₄ array grown on Ni foam for the Simultaneous Electrochemical Detection of Copper(II) and Mercury(II)

Shushan Yao^{1,2}, Lifei Zhi^{1,2}, Jin Guo^{1,2}, Shijian Yan^{1,2}, Mingang Zhang^{1,2*}.

¹ Institute of Advanced Materials, Taiyuan University of Science and Technology, Taiyuan 030024, Shanxi, P. R. China.

² School of Materials Science and Engineering, Taiyuan University of Science and Technology, Taiyuan 030024, Shanxi, P. R. China.

*E-mail: mgzhang07@163.com

Received: 30 September 2017 / Accepted: 16 November 2017 / Published: 16 December 2017

Hierarchical porous NiCo₂O₄ array grown on Ni foam (NiCo₂O₄/NF) was synthesized by a facile one-step hydrothermal reaction and then directly applied as the binder-free electrode of electrochemical sensor. Impressively, the NiCo₂O₄/NF exhibited rapid detection and high sensitivity for simultaneous electrochemical detection of copper and mercury ions, in which the sensitivity was about 29.8 μA/μM and 23.7 μA/μM, respectively. Moreover, it also showed good repeatability and long-term stability (2.4% decrease in response over 10 testing times and 30 days). This work did not only provided a facile method of synthesis hierarchical porous NiCo₂O₄/NF, but also proved that the hierarchical porous layered double hydroxides could be applied in simultaneous electrochemical detection of heavy metal ions.

Keywords: NiCo₂O₄ microflowers, Hierarchical porous, Metal determination, Electrochemical sensor.

1. INTRODUCTION

It was well-known that environmental issues were one of the biggest global challenges in the new century[1]. Especially, with the rapid growth of worldwide industry, heavy metal ions in water have already become serious problem, which affected the human healthy and the survival environment of creatures[2]. Therefore, sensitive determination of toxic heavy metal ions with a cost-effective and convenient procedure was paramount important. Electrochemical detection method has attracted lots of interests due to its simplicity, low cost and high sensitivity comparing to other methods[3-4]. So, the development of nanomaterials based sensor was the key for the application of electrochemical

detection method[3-10]. Although a lot of works have reported on electrochemical detection heavy metal ions, only a few works reported the simultaneous electrochemical sensing several target metal ions[10]. In recent years, spinel nickel cobaltite (NiCo_2O_4) nanomaterials have attracted increasing attention in electrode material of energy storage and electrochemical analytical science due to be high electrochemical activity, low cost, environmental friendliness and abundant resources[11-17]. Generally, electrode materials with hierarchical porous array structures exhibited higher electrochemical performance comparing to powder or others array structures[18-20]. However, up to now, the electrochemical sensors based on hierarchical porous NiCo_2O_4 array were few reported, especially for simultaneous electrochemical sensing several target metal ions in water.

In this work, hierarchical porous $\text{NiCo}_2\text{O}_4/\text{NF}$ was synthesized by facile hydrothermal and thermal decomposition process and was directly applied in heavy metal sensor. This work firstly explored the application of $\text{NiCo}_2\text{O}_4/\text{NF}$ in the simultaneous electrochemical detection of heavy metals ion. Moreover, it revealed high sensitivity, low detection limit for simultaneous electrochemical detection heavy metals, which was expected to application in the future.

2. EXPERIMENT

2.1 Preparation of hierarchical $\text{NiCo}_2\text{O}_4/\text{NF}$

$\text{NiCo}_2\text{O}_4/\text{NF}$ was synthesized via a one-step hydrothermal approach followed by annealing in air. All chemical reagents were of analytical purity and use without further purification. The Ni foam (approximately $1.0\text{cm} \times 2.0\text{cm}$) were cleaned by ultrasonication in 3 M HCl aqueous solution to remove the NiO layer, then washed carefully with absolute ethanol and deionized water for 30.0min. In a typical procedure, $\text{Co}(\text{NO}_3)_2 \cdot 6\text{H}_2\text{O}$ (0.384g, 1.32mmol), $\text{Ni}(\text{NO}_3)_2 \cdot 6\text{H}_2\text{O}$ (0.192g, 0.366mmol), urea (1.204g, 20.0mmol), NH_4F (0.296g, 8.0mmol) were dissolved in deionized water (40.0ml), and stirred to form a homogeneous pink solution. Then the solution and the Ni foam was transferred into 50.0ml Teflon-lined stainless steel autoclave. The temperature of hydrothermal was set at 100.0°C for 6.0h. After it was cooled down to room temperature, the red product on Ni foam was taken out and then washed with deionized water and ethanol, dried at 60.0°C for 12.0h, and then calcined at 300.0°C in air for 2.0h.

2.2 Material characterization

The crystalline structure of the product was examined by a Bruker D8 Avance X-ray diffractometer using Cu K α radiation at a scan rate of $5^\circ/\text{min}$.

The morphology of product was investigated by a field emission transmission electron microscope (TEM, JEOL 2100) and by a field emission scanning electron microscope (FESEM, Hitachi S-4800). The element composition was characterized by a Horiba EX-250 X-ray energy-dispersive spectrometer (EDS) associated with SEM.

The Cu and Hg element in water was determination by an ICP-MS (Elan DRC II, Perkin Elmer,

Norwalk, CT). The ICP operating conditions were shown in following: RF power of 1100W, Ar nebulizer gas flow of 0.6-0.9L min⁻¹ and Scan mode of Peak hopping.

2.3 Electrochemical characterization

All electrochemical measurements (electrochemical impedance spectroscopy (EIS), cyclic voltammetry (CV) and differential SWASV) were performed on a CHI1140A electrochemical workstation (CHI110, Austin, TX). The NiCo₂O₄/NF with 1.0cm×2.0cm, Pt-wire and Ag/AgCl electrodes were used as working, counter and reference electrodes, respectively. All electrochemical measurements were carried out at room temperature.

Hg (II) and Cu(II) were analyzed by differential SWASV. A preconditioning of the NiCo₂O₄/NF was carried out before each analysis by recording ten CV from 0 to +0.8V at a scan rate of 100.0mV s⁻¹ in electrolyte solution (0.1M HCl). The NiCo₂O₄/NF was immersed in 25.0mL magnetically stirred standard solution or sample and Hg (II) and Cu(II) were reduced to Hg (0) and Cu (0) by applying a potential of -1.1V for 180.0s. Then, the electrode was rinsed with distilled water and transferred to another cell that contained of 25.0mL 0.1M HCl. Hg (II) and Cu(II) analysis was carried out by SWASV from -1.1V to 0.8V with 10.0mV s⁻¹ scan rate, 25.0mV modulation amplitude, 50.0ms modulation time and 5.0mV step potential.

3. RESULT AND DISCUSSION

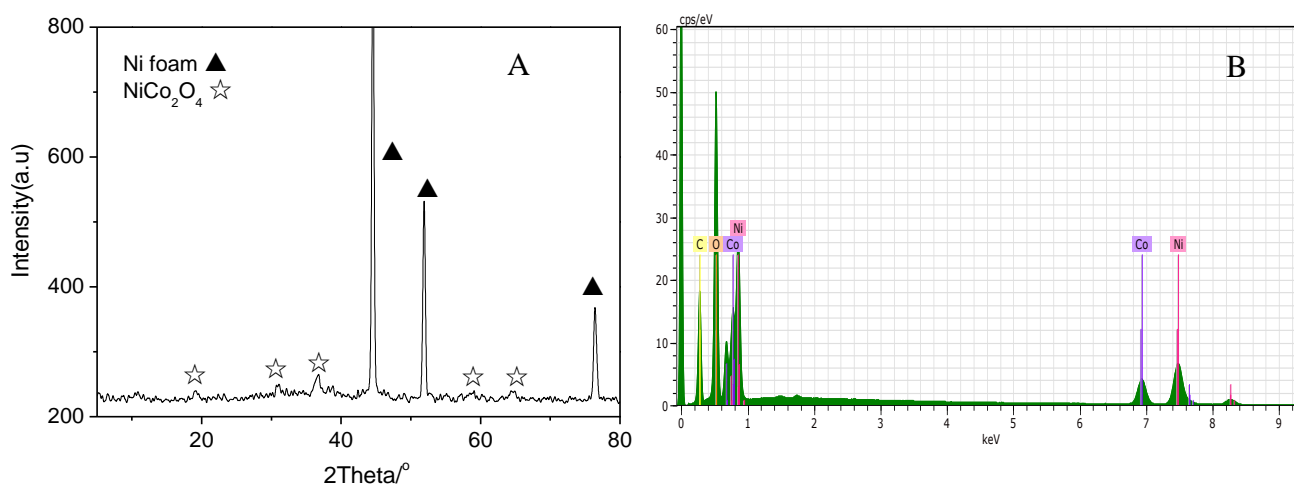


Figure 1. (A) XRD and (B) EDS spectrum of NiCo₂O₄/NF.

The XRD of NiCo₂O₄/NF was firstly characterized as shown in Fig.1A. It clearly showed three sharp peaks at 44.4°, 51.8° and 76.3°, corresponding to the diffractions of (111), (200) and (220) planes of Ni, respectively (JCPDS card No. 04-0850) [21]. In addition to this, there was others diffraction peaks at 18.9°, 30.8°, 36.8°, 59.0° and 64.8°, which were assigned to (111), (220), (311), (511) and (440) planes of NiCo₂O₄, respectively (JCPDS card No. 73-1702) [11]. These results indicated the formation of NiCo₂O₄/NF. To determine the elemental compositions of NiCo₂O₄ grown on Ni foam, energy dispersive spectroscopy (EDS) analysis was also carried out as shown in Fig. 1B. The pattern

peaks of Co, Ni and O were clearly observed in the spectrum, indicating the existence of the elements. Moreover, the corresponding molar ratio of Ni:Co:O was determined to be about 1.00:1.98:4.05, which was consistent with the formula of NiCo_2O_4 [17]. The EDS results further confirmed the formation of $\text{NiCo}_2\text{O}_4/\text{NF}$.

The microstructure of $\text{NiCo}_2\text{O}_4/\text{NF}$ was characterized by the SEM images as shown in Fig.2A-C. It clearly showed lots of microflowers with a average diameter of $11.0\mu\text{m}$, which uniformly grew on the backbones of the Ni foam as shown in Fig.2A-B. By a closer examination, the microflowers were composed of 2D nanosheets with the thickness and diameter of about 50.5nm and $2.0\mu\text{m}$, respectively as shown in Fig.2C. To further confirm the architecture of NiCo_2O_4 microflowers grown on Ni foam composed of nanosheets, which was further characterized by the TEM image as shown in Fig.2D. It displayed a view of a whole nanosheets. At the same time, it was a single nanocrystal, which showed polycrystalline in nature. These results confirmed the formation of hierarchical porous NiCo_2O_4 microflower array grown on Ni foam. The hierarchical porous array provided more channels and active surface area for penetrating metal ions to the inner of active materials and thus accelerating the interfacial reaction with active materials. These were benefit to improve the properties of electrochemical detection[22].

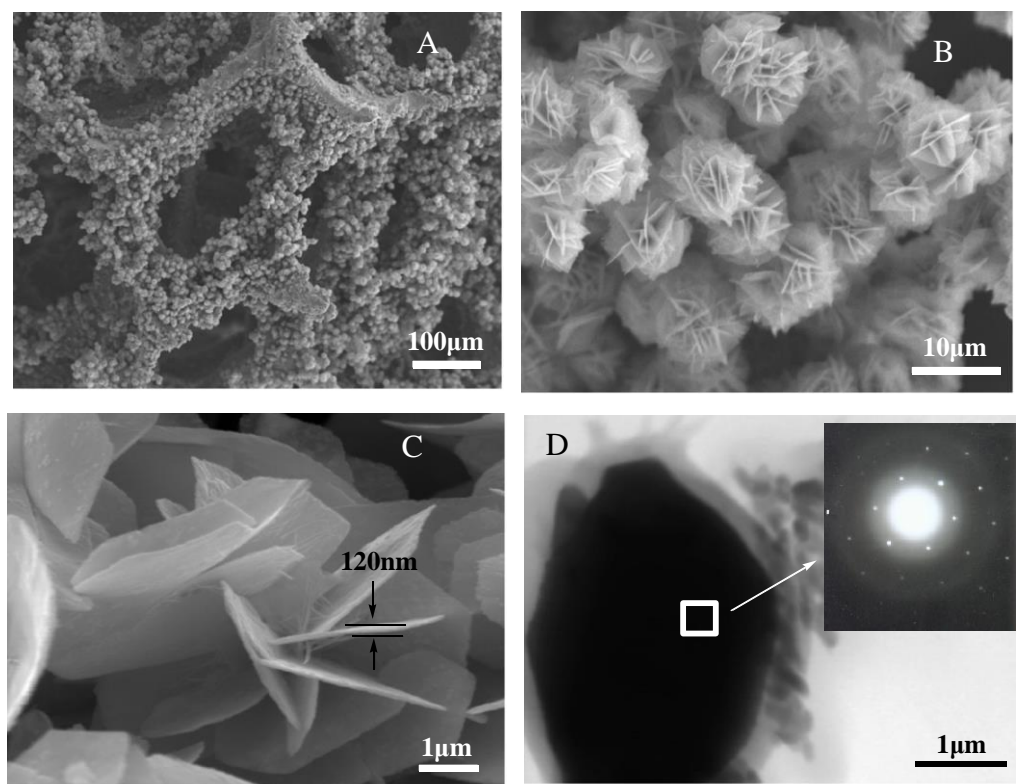


Figure 2. (A-C) SEM images of the $\text{NiCo}_2\text{O}_4/\text{NF}$, (D) TEM image of the NiCo_2O_4 nanosheet. The inset of (D) was the SAED pattern of NiCo_2O_4 nanosheet.

The CV responses of pure Ni foam and $\text{NiCo}_2\text{O}_4/\text{NF}$ were displayed and compared in Fig.3A . It clearly showed that the anodic and cathodic peak currents of the $\text{NiCo}_2\text{O}_4/\text{NF}$ were higher than that of the pure Ni foam. The result was contributed to the NiCo_2O_4 grown on Ni foam [18]. In addition to

this, the result also suggested that the NiCo₂O₄/NF was better electrochemical catalytic behavior and promotion of electron transfer process comparing to pure Ni foam. The interface property of the pure Ni foam and NiCo₂O₄/NF was also characterized and compared by the EIS spectrum as shown in Fig.3B. The equivalent series resistance (ESR) of NiCo₂O₄/NF was slight red shit comparing to pure Ni foam. Yet, the charge transfer resistance (R_{ct}) of NiCo₂O₄/NF obviously increased comparing to the pure Ni foam. These results suggested that the NiCo₂O₄ coatings resulted in larger ohmic drop with respect to the pure Ni foam [23].

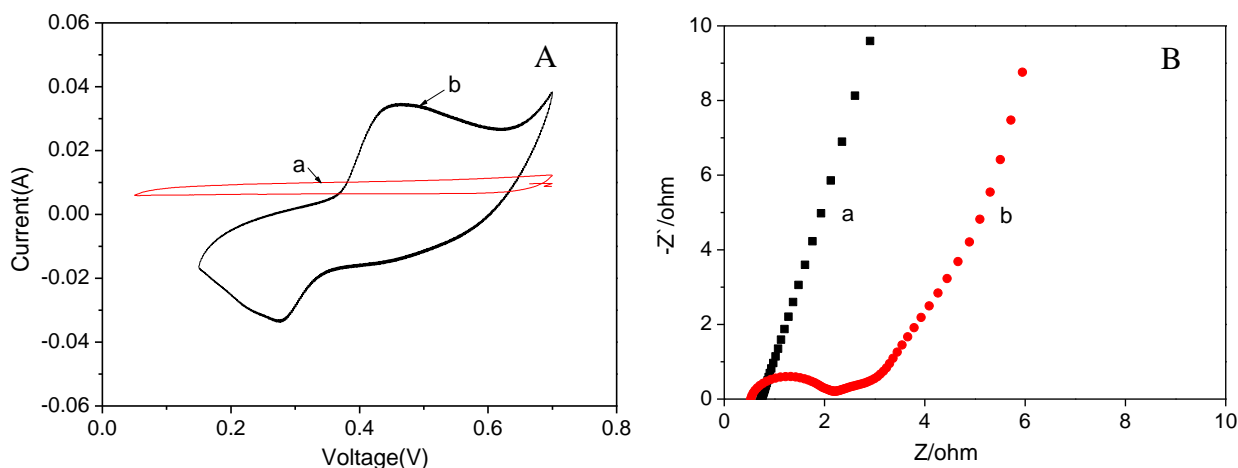


Figure 3. (A) cyclic voltammetric responses and (B) electrochemical impedance spectra of (a) pure Ni foam and (b) NiCo₂O₄/NF.

Under the optimal experimental conditions, Hg(II) and Cu(II) was simultaneously determined on NiCo₂O₄/NF using SWASV as shown in Fig.4. Fig.4A clearly showed the SWASV response of the NiCo₂O₄/NF toward Hg(II) and Cu(II) over the concentration range of 0.8 to 2.8 μ M. The calibration plot of Hg(II) and Cu(II) was further calculated as shown in Fig.4B, in which the peak currents increased linearly versus the Hg(II) and Cu(II) concentrations. The limit of detection (LOD) for simultaneous detection Hg(II) and Cu(II) was about 0.00991 μ M and 0.0115 μ M (3 σ method), respectively. Moreover, the high sensitivity (ca.29.8 μ A/ μ M and 23.7 μ A/ μ M) of simultaneous detection Hg(II) and Cu(II) was obtained, respectively.. These results indicated that the Hg (II) and Cu(II) ions in water could be simultaneously detected in complex samples with minimum interference. By comparing the sensitivity and LOD of other electrodes based on Ni foam or NiCo₂O₄ for electrochemical detection, it was found that the NiCo₂O₄/NF exhibited largest sensitivity as shown in Table 1. These results demonstrated that the NiCo₂O₄/NF could be as free-standing electrochemical electrode applied in simultaneous electrochemical detection of Hg and Cu heavy metal ions. Furthermore, it showed high sensitivity for simultaneous electrochemical detection of Hg and Cu ions in water. The simultaneous electrochemical detection property might be attributed to that a couple of redox reaction of Co³⁺/Co⁴⁺ and Ni²⁺/Ni³⁺ transitions associated with metal ions was reversible. And the high high sensitivity was attributed to the hierarchical porous structure of NiCo₂O₄ grown on Ni foam, which could offer a large active surface area and more active sites to be accessed by metal ion, and enabled rapid ion transport.

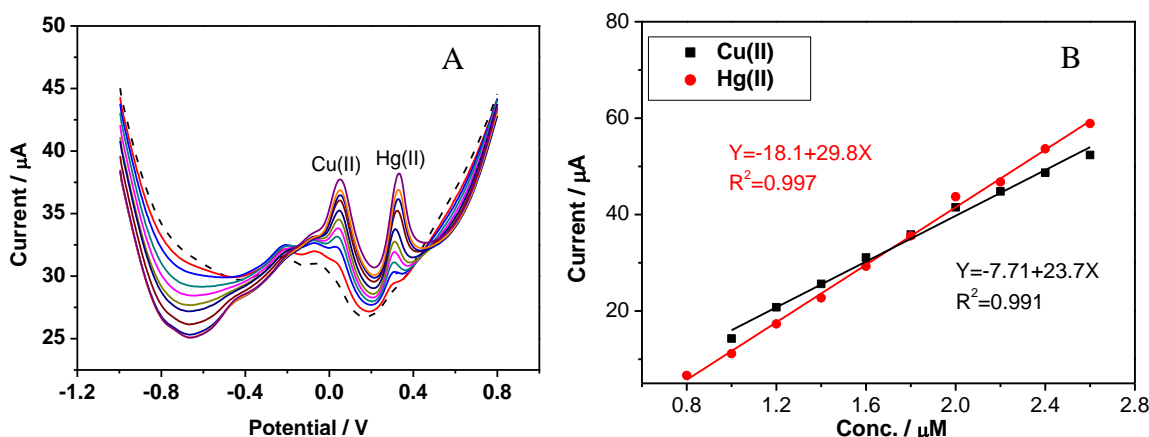


Figure 4. (A)SWASV responses and (B) the corresponding calibration plots of NiCo₂O₄/NF towards Hg(II) and Cu(II) at different concentrations in 0.1 M HCl solution.

Table 1. Comparison of current sensitivity and LOD with previously reported values of different electrodes.

| Electrodes | Sensitivity ($\mu\text{A}/\mu\text{M}$) | LOD (μM) | Detection materials | Ref. |
|---|---|-----------------------|---------------------|---------|
| NiCo ₂ O ₄ /NF | 29.8 | 0.00991 μM | Hg(II) | present |
| (Simultaneous) | 23.7 | 0.0115 μM | Cu(II) | |
| SnO ₂ /RGO powder | 2.713 | 0.1220nM | Hg(II) | [24] |
| (Simultaneous) | 9.664 | 0.03390nM | Cu(II) | |
| (Co,Mn) ₃ O ₄ /Ni foam | 6.91 | 0.013 μM | Hg(II) | [19] |
| Ag/rGO foam | 8.0 | 0.11 μM | Hg(II) | [18] |
| NiCo ₂ O ₄ /citrate powder | 0.2397 | 5.4pM | Eugenol | [17] |
| NiCo ₂ O ₄ /Au/organic molecules powder | ----- | 0.5pg/ml | Immunosensor | [16] |

Generally, the metal oxides powder were coated on the glass carbon electrode for electrochemical detection, which showed poor stability[23]. The problem restricted its practical applications. Here, the stability of NiCo₂O₄/NF for electrochemical detection was evaluated by SWASV responses toward Hg(II) solution with the concentration 0.9 μM as function of cycling test and storage time as shown in Fig.5A. It clearly showed that the peak current slightly changed with increase in cycling test and storage time. Furthermore, it became stable after 10 cycling tests and

storage 30 days, in which the peak current only decreased to be 2.4% comparing to initial peak current. The result suggested that the NiCo₂O₄/NF with hierarchical porous structure exhibited a good cycling stability and long-term durability [24]. The good cycling stability and long-term durability was showed following two reasons. (1) NiCo₂O₄ was grew on Ni foam, which had strong interface between active materials and electrode, (2) the NiCo₂O₄ was hierarchical porous structure, which provided the free volume for cubic expansion of active materials during electrochemical process. In order to confirm mechanism of high cycling stability, the EIS of NiCo₂O₄/NF before and after 10 cycling tests was also determined and compared as shown in Fig.5B. There was slight change in ESR and Rct before and after 10 cycling tests. The result indicated that the effect of cycling tests on structure of the NiCo₂O₄/NF was slight.

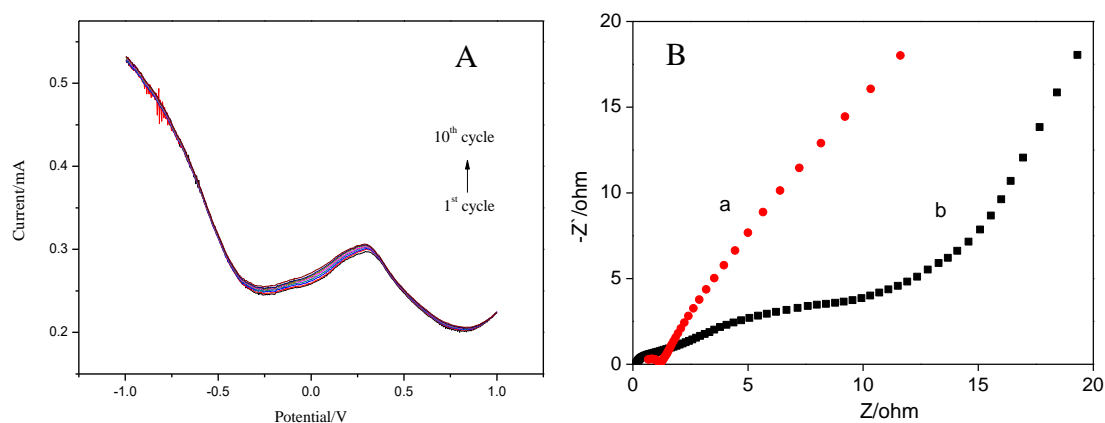


Figure 5. (A) SWASV responses and (B) EIS of NiCo₂O₄/NF toward Hg(II) from 1st cycle to 10th cycle.

To demonstrate the practical application of the NiCo₂O₄/NF, Cu(II) and Hg(II) with known amount was added to tap and lake water. The two samples were filtered through a 0.3µm membrane before detection. In a comparison, the two samples were also analysis by inductively coupled plasma technology (ICP). These results were concluded and compared in Table 2, in which the electrochemical analysis (EA) results were statistical data for five determinations. It clearly showed that the EA results were similar with the ICP results, which was generally to determine the concentration of metal in water. Furthermore, the average recoveries of Cu(II) and Hg(II) ranged from 100.8% to 96.0% and 110.0% to 104.6%, respectively. These results indicated that the NiCo₂O₄/NF as electrode of electrochemical sensor was good accuracy for simultaneous detection Cu(II) and Hg(II) in the real-world samples.

Table 2. Simultaneous determination of Cu(II) and Hg(II) in water samples

| Sample | | Added (µM) | ICP result (µM) | EA result (µM) | Recovery (%) |
|------------|--------|------------|-----------------|----------------|--------------|
| Tap water | Cu(II) | 0.5 | 0.49 | 0.48±0.03 | 96.0 |
| | Hg(II) | 0.1 | 0.10 | 0.11±0.02 | 110.0 |
| Lake water | Cu(II) | 2.5 | 2.46 | 2.52±0.13 | 100.8 |
| | Hg(II) | 3.0 | 3.10 | 3.14±0.11 | 104.6 |

4. CONCLUSION

Hierarchical porous NiCo₂O₄/NF was successfully synthesized by a one-step hydrothermal approach. Furthermore, it could act as the binder-free electrode for the simultaneous detection of Hg(II) and Cu(II) due to be reversible redox reaction of Co³⁺/Co⁴⁺ and Ni²⁺/Ni³⁺ transitions associated with metal ions. And it showed simultaneously high sensitivity of 29.8μA/μM and 23.7μA/μM due to be Hierarchical porous structure. These findings provided a new ground to design and preparation electrode materials for simultaneous electrochemical sensing several target metal ions in real water.

ACKNOWLEDGMENTS

The authors are grateful for Shanxi Science and Technology Foundation Platform Construction Projects (2015091011) Jincheng Science and Technology Planning Projects(201501004-21). The authors acknowledge Research follow Qiang Fu from University of Melbourne for assistance English edition.

References

1. M.B.Gumpu, S.Sethuraman and U.MaheswariKrishnan, *Sensors and Actuators B: Chemical*, 213(2015)515.
2. L.Cui, J.Wu and H.X.Ju, *Biosensors and Bioelectronics*, 63(2015)276.
3. G.Aragay and A.Merkoçi, *Electrochimica Acta*, 84(2012)49.
4. G.Zhao, H.Wang and G. Liu, *Int. J. Electrochem. Sci.*, 12 (2017) 8622.
5. L.Xiao, G.G. Wildgoose, R. G. Compton, *Analytica chimica acta*, 620(2008)44.
6. G. Aragay, J. Pons and A. Merkoçi, *J. Mater. Chem.*, 21(2011)4326.
7. S.I.Ting, S.J. Ee, A.Ananthanarayanan and K.C. Leong, *Electrochimica Acta*, 172(2015)7.
8. D. Bagchi, T.K. Maji, S.Sardar, P. Lemmens, C.Bhattacharya, D. Karmakar and S.Kumar Pal, *Phys. Chem. Chem. Phys.*, 19(2017)2503.
9. S.F.Zhou, J.J.Wang, L. Gan, X.J.Han,H.L.Fan, L.Y.Mei, J.Huang and Y.Q.Liu, *Journal of Alloys and Compounds*, 721(2017)492.
10. S. Deshmukh, Ga.Kandasamy, R. K.Upadhyay, G.Bhattacharya, D.Banerjee, D. Maity, M.A.Deshusses and S.S.Roy, *Journal of Electroanalytical Chemistry*, 788(2017)91.
11. J.Guo, Z.H.Yin, X.X.Zang, Z.Y.Dai, Y.Z.Zhang, W. Huang and X.C.Dong, *Nano Research*, 10(2017)405.
12. T.Han, C.X. Wang, J.R. Yao, J.L.Jin, Y.Y. Sun, Y.H.Zhang and Y.Q. Liu, *Int. J. Electrochem. Sci.*, 12 (2017) 4724.
13. S.Q.Cui, L.Li,Y.P.Ding, J.G.Zhang, H.Yang and Y.Z.Wang, *Talanta*, 164(2017)291.
14. J.J.Zhang, Q.W. Mei, Y.P. Ding, K.Guo, X.X.Yang and J.T.Zhao, *ACS Appl. Mater. Interfaces*, 9(2017)29771.
15. S.Q.Cui, J.J.Zhang,Y.P.Ding, P.Hu and Z.Q.Hu, *Science China Materials*, 60(2017)766.
16. Q.F.Li, L.X.Zeng, J.C.Wang, D.P.Tang, B.Q. Liu, G.N.Chen and M.D.Wei, *ACS Appl. Mater. Interfaces*, 3(2011)1366.
17. M.U. Anu Prathap, C.Wei, S.N.Sun and Z.C.Xu, *Nano Research*, 8(2015) 2636.
18. T. Han, J.J. Jin, C.X. Wang, Y.Y.Sun, Y.H. Zhang and Y.Q.Liu, *Nanomaterials*, 7(2017)40.
19. J. Ma,W.H.Zhang, L.Zheng, Y.Y.Sun, R.Y. Jin, G.Z. Zhao and Y.Q. Liu, *Journal of Alloys and Compounds*, 663(2016)230.

20. Y.Y.Sun, W.H.Zhang, D.S. Li, L.Gao, C.L. Hou, Y.H. Zhang and Y.Q.Liu, *Electrochimica Acta*, 178(2015)823.
21. S.Y.Hao, Y.Y.Sun, Y.Q.Liu, Y.H.Zhang and G.S.Hu, *Journal of Alloys and Compounds*, 689(2016)587.
22. X.J. Du, W.G.Wu, C.H.An, Y.P.Cheng, X.Y.Zhang, Y.Y. Sun and Y.Q. Liu, *Int. J. Energy Res*, 40(2016)1731.
23. Y.Y. Sun, W.H.Zhang, D.S. Li, L. Gao, C.L. Hou, Y.H. Zhang and Y.Q.Liu, *Journal of Alloys and Compounds*, 649(2015)579.
24. Y. Wei, C.Gao, F.L.Meng, H.H. Li, L.Wang, J.H.Liu and X.J.Huang, *J. Phys. Chem. C.*, 116(2012)1034.

© 2018 The Authors. Published by ESG (www.electrochemsci.org). This article is an open access article distributed under the terms and conditions of the Creative Commons Attribution license (<http://creativecommons.org/licenses/by/4.0/>).